

IN-SITU INERTIAL CHARACTERIZATION OF A SAW-BULK GYROSCOPE

A Design Project Report

Presented to the School of Electrical and Computer Engineering
of Cornell University
in Partial Fulfillment of the Requirements for the Degree of
Master of Engineering, Electrical and Computer Engineering

Submitted by

Paolo Arguelles

MEng Field Advisor: Professor Amit Lal

Degree Date: May 2019

© 2019 SonicMEMS Research Laboratory, Cornell University
ALL RIGHTS RESERVED

ABSTRACT

Master of Engineering Program

School of Electrical and Computer Engineering

Cornell University

Design Project Report

Project Title: *In-Situ* Inertial Characterization of a SAW-Bulk Gyroscope

Author: Paolo Arguelles

Abstract:

Often referred to as Coriolis vibratory gyroscopes (CVGs), most commercially available microelectromechanical systems- (MEMS) based gyroscopes are comprised of a moving, resonating spring-mass system, making use of the Coriolis effect to sense multiple degrees of freedom. While widely used and practical for most consumer use, such devices are often unreliable when used in special defense and military applications where extreme forces and accelerations are present. The purpose of this project is to develop a MEMS gyroscope suitable for placement on high-velocity ballistics. Using bulk-micromachining and surface acoustic wave (SAW) technology, the SonicMEMS Laboratory at Cornell University aims to fabricate a solid-state version of the conventional MEMS gyroscope on piezoelectric, lithium niobate substrate, intended for use in advanced inertial micro-sensing for high-velocity munitions.

BIOGRAPHICAL SKETCH

Paolo Arguelles is a candidate for the Master's Degree in the School of Electrical and Computer Engineering at Cornell University.

He began college at the age of 14, and soon after received his Bachelor's Degree in Electrical Engineering from California State University, Los Angeles, graduating *summa cum laude*. He was named by the Honors College as an Edison Scholar in 2014 and was honored by the Barry Goldwater Scholarship committee in 2016 for his research proposal on black holes. He served as president of the Early Entrance Program Club and campus chair of the Institute of Electrical and Electronics Engineers (IEEE). He is a proud member of the honor societies of Phi Kappa Phi and Tau Beta Pi.

Paolo began graduate study at Cornell University at the age of 19. In addition to conducting his present thesis work on a surface and bulk acoustic wave gyroscope with the SonicMEMS Laboratory under the guidance of Professor Amit Lal, he is a member of the Collective Embodied Intelligence Laboratory under Assistant Professor Kirstin Petersen where he conducts research work in bio-inspired swarm robotics. He is also a researcher at Cornell's Space Systems Design Studio (SSDS) under Professor Mason Peck, where he developed the software and electrical subsystems for the Attitude Testbed and Spacecraft Flight Simulator (ATTEST).

After Cornell, Paolo plans to enjoy a gap year before embarking on new and exciting adventures and challenges.

This work is dedicated to all the professors, faculty, and friends who have
made my time at Cornell memorable.

EXECUTIVE SUMMARY

This research effort aims to develop a solid-state gyroscope based on bulk and surface acoustic wave technology. This monolithic approach offers several advantages over the conventional released mass MEMS architecture, including increased tolerance to high shock environments, as well as a higher dynamic range.

An *in situ* measurement scheme was implemented using the Moku:Lab, a commercial off-the-shelf instrument. MATLAB scripts interface with both the Moku:Lab configured as a lock-in amplifier, and the temperature-controlled inertial rate table to conduct a variety of inertial tests and collect the resulting data. A double demodulation scheme is used to first perform an *in situ* demodulation step in the Moku:Lab hardware to separate the frequency component due to the drive frequency of the gyroscope, and an additional demodulation step is performed digitally to extract the gyroscopic response of the device. Both SAW and bulk modes were found using this new, integrated setup.

While further investigation of gyroscopic scale factor at each detected mode is needed to determine whether the sample functions as a gyroscope, these results contained in this report clearly indicate the device's veritability as a solid-state inertial sensor. Code listings and step-by-step procedures detailing the operation of the MATLAB programs are provided in the appendices.

TABLE OF CONTENTS

Biographical Sketch	iii
Dedication	iv
Executive Summary	v
Table of Contents	vi
List of Figures	vii
1 Project Overview	1
1.1 Statement of Work (SOW)	1
1.2 Work Breakdown Structure (WBS)	2
2 Background and Theory	3
2.1 Gyroscopes and the Coriolis Force	3
2.2 Surface and Bulk Acoustic Waves	7
2.2.1 Using SAW and BAW to Measure Rotation in a Gyroscope	7
3 Experimental Methods	11
3.1 Testbed Integration	11
3.2 Isolating Gyroscopic Response with Double Demodulation	14
3.3 Results	18
3.3.1 Sources of Noise	20
4 Conclusion	23
References	25
A Suggested Experimental Procedures	26
A.1 Detecting SAW Modes	26
A.2 Detecting Bulk Modes	27
A.3 Determining Scale Factor	28
B Moku:Lab MATLAB Interface Code Listings	30
C Post-Processing MATLAB Code Listings	36

LIST OF FIGURES

2.1	A conventional single-axis released mass gyroscope	6
3.1	PASCO Mechanical Wave Driver	11
3.2	Proposed integrated setup	12
3.3	Test setup mounted on rate table	13
3.4	Fully integrated Moku:Lab testing framework	14
3.5	Double demodulation scheme	15
3.6	Detected bulk modes	18
3.7	SAW modes detected with Moku:Lab setup	19
3.8	Temperature driven low frequency oscillations	21

CHAPTER 1

PROJECT OVERVIEW

The aim of this project is to develop a high-shock solid-state gyroscope for military-grade applications using surface and bulk acoustic wave (SAW/BAW) technology. This research work operates under the auspices of DARPA's High Operational Rate and Shock Environment SAW Inertial Sensors (HORSES) program.

1.1 Statement of Work (SOW)

Phase I: Inertial Integrated Testbed The candidate shall create a testing scheme that incorporates a single-axis rate table and lock-in amplifier in a temperature-controlled environment. This necessitates the creating of a 3D printed mount that suspends the sample directly above the center of rotation of the rate table.

Phase II: Characterization of Gyroscopic Behavior The candidate shall characterize the behavior of the SAW device by conducting frequency sweeps in conjunction with inertial tests to attempt to demonstrate gyroscopic behavior. Since the nature and requirements for this project flow from ongoing research, these guidelines are purposely left nebulous and open to change as the project team sees fit.

Program Management All work and findings related to this project are subject to external regular review by DARPA program management. Internal review meetings and progress reports are conducted on a regular basis with

principal investigator Professor Amit Lal, Benyamin Davaji, and Visarute Pinrod.

1.2 Work Breakdown Structure (WBS)

Table 1.1: Work Breakdown Structure

WBS	Task
1.0	Phase 1 - INTEGRATED INERTIAL TESTBED
1.1	Study prior research in the field, particularly previous SonicMEMS work
1.2	Become fluent in PyMoku/moku-MATLAB interfaces
1.3	Design and print mount for SAW gyro
2.0	Phase 2 - GYROSCOPE CHARACTERIZATION
2.1	Measure S_{21} parameter using integrated setup
2.2	Develop MATLAB code to interface with Moku:Lab and rate table
2.3	Create first demodulation plots
2.4	Develop MATLAB code to conduct digital demodulation
2.5	Create second demodulation plots
2.6	Determine gyroscopic scale factor

CHAPTER 2

BACKGROUND AND THEORY

2.1 Gyroscopes and the Coriolis Force

The architectures of gyroscopic sensors usually rely on the *Coriolis effect*, a fictitious force used to describe the motion of objects within a frame of reference rotating with respect to another frame of reference. A relatable real-world analogy for the Coriolis effect consists of imagining a car traveling along a straight highway. Although it would be obvious to an outside observer outside the inertial frame of the car (i.e. a pedestrian on the side of the road) that the car is moving, as far as its occupants are concerned, they are stationary, that is, as long as the car is not accelerating. When the car encounters a sharp bend in the road, the inertial tendency of the driver is to continue along the straight path. However, when the car is defined as the frame of reference, as is the case for its occupants, the driver appears to be thrust to one side due to an invisible force. Unless the greater context of a sudden turn is provided to the occupants in the car (i.e. looking out the window) the cause of this force is unapparent to observers.

This force, called the centrifugal force, is one of the fictitious forces invoked to explain the effects of inertia for observers in an accelerating, rotating, inertial frame of reference. Given the existence of the centrifugal force, imaging trying to throw a ball from the back seat of the car to hit the rear view mirror directly along the middle axis of the vehicle. For a car traveling straight, this is a trivial task. However, when the ball is thrown mid-turn, the observer throwing the ball will see that the ball skews away from its expected (straight) trajectory in

the direction of the centrifugal force. This “skew” is attributable to the Coriolis force, and the apparent change in trajectory as a result of this force is called the Coriolis effect. The Coriolis effect is the fundamental principle underlying the operation of all gyroscopic sensors.

The effect may be characterized mathematically by first invoking Newton’s Second Law of Motion.

$$F = ma \quad (2.1)$$

This formula is a simplification of Newton’s Law, as it only applies to non-accelerating frames. Transforming Newton’s Second Law into a rotating inertial frame of reference yields additional terms,

$$F - m \frac{d\Omega}{dt} \times r - 2m\Omega \times v' - m\Omega \times (\Omega \times r) = ma' \quad (2.2)$$

each corresponding to a “fictitious force” invoked to describe motion in a rotating frame:

$$F + F_{Euler} + F_{Coriolis} + F_{centrifugal} = ma' \quad (2.3)$$

The Coriolis force component is described by:

$$F_c = -2m\Omega \times v' \quad (2.4)$$

The magnitude of the acceleration induced by the Coriolis effect is then:

$$a_c = 2(\Omega \times v') \quad (2.5)$$

The goal of the gyroscope is to extract rate of rotation Ω . The angular position,

or absolute orientation, of the sensor may then be derived by accumulating (i.e. integrating) this output over time. One straightforward way to do this is to examine the effect of rotation on a known mass. Consider a mass m driven back and forth on its drive axis, whose drive-plane position is described by:

$$x_d(t) = \sin(\omega_d t) \quad (2.6)$$

where ω_d is the drive frequency of the proof mass. Then its drive-plane velocity is:

$$v(t) = \omega_d \cos(\omega_d t) \quad (2.7)$$

Its sense-plane motion, induced by the Coriolis effect, may then be described as:

$$x_s(t) = \frac{F_c}{k_{sense}} = m \frac{a_c}{k_{sense}} = \frac{2m\Omega\omega_d \cos \omega_d t}{k_{sense}} \quad (2.8)$$

where k_{sense} is the effective spring constant of the combination of cantilever beams supporting motion in the sense axis. It should be noted here that the proof mass must vibrate in order for the system to function as a gyroscope. If no vibrations are applied, the proof mass is susceptible to linear accelerations, effectively making the sensor an accelerometer.

Such systems may be implemented at the MEMS level, creating micro-size gyroscopes. These types of conventional MEMS gyroscopes are known as Coriolis vibratory gyroscopes due to their reliance on the Coriolis effect. As shown above, Coriolis vibratory gyroscopes sense orientation by driving, or vibrating, a proof mass back and forth inside a frame. When an external angular rate is applied to the system, the Coriolis force causes the proof mass to deviate from its

linear trajectory and skew along the axis lateral to its vibratory mode. When the proof mass is perturbed in this manner, a sensing finger attached to the proof mass is displaced from the center of an electrode pair, changing the capacitance between the finger and each electrode (Figure 2.1).

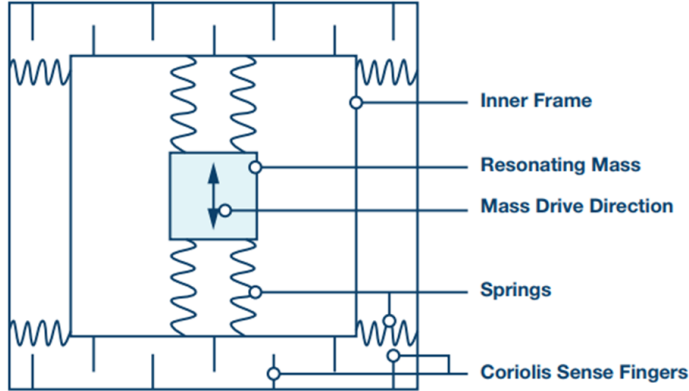


Figure 2.1: A conventional single-axis released mass gyroscope

This scheme has largely been reliable for daily consumer use, variants of which have been used in smartphones, gaming devices, and cameras. However, when using conventional MEMS-based gyroscopes for inertial sensing in high-shock environments, such as in military-grade applications, extreme forces may break the delicate structures that suspend the proof mass, rendering the device unusable. For many such markets, there exists a clear need for a monolithic, solid-state version of the Coriolis vibratory gyroscope that is able to withstand high-shock environments. The current project posits that such a gyroscope may be implemented using surface and bulk acoustic wave- (SAW/BAW) based technology.

2.2 Surface and Bulk Acoustic Waves

Surface acoustic waves (SAW) are mechanical perturbations (i.e., sound waves) that travel along the surface of a material exhibiting elasticity. Their amplitude decays into the bulk of the substrate, the axis transverse to the direction of propagation. In the present case, SAWs are generated by interdigitated transducers (IDTs), a special kind of transducer whose electrodes are periodic and interdigitated. The electrode pitch spacing of one terminal is consistent with the desired SAW wavelength λ_{SAW} . Bulk acoustic waves (BAWs) differ from SAWs in that its primary direction of propagation is in the bulk of the substrate.

2.2.1 Using SAW and BAW to Measure Rotation in a Gyroscope

Recall that SAW and BAW modes operate due to standing wave resonators in the surface and bulk of an elastic substrate, respectively. Since these axes are orthogonal to each other, coexisting SAW and BAW effects may be used to conduct multi-axis inertial sensing in a single solid-state gyroscope.

SAW Mode

SAW gyroscopes use IDTs to convert a sinusoidal voltage into acoustic energy, which propagates throughout the sensor substrate. Reflectors are positioned throughout the substrate causing standing waves to form a resonating cavity. To sense orientation, metallic dots are dispersed around the center of the sensor such that they are located at the antinodes of the SAW standing waves. This set of masses, known as a distributed Coriolis mass array (DCMA) produces aux-

iliary surface acoustic waves proportional to the Coriolis force experienced by each metallic dot [1, 2]. These auxiliary waves are sensed by another pair of IDTs and converted into an analog electrical signal, which may then be interpreted as an angular rate.

The masses are distributed on the surface of a lithium niobate (LiNbO_3) substrate, an elastic, piezoelectric material. As in the CVG architecture, these masses are driven in and out of the plane of the substrate. This may be achieved by applying a sinusoidal voltage to an interdigitated transducer (IDT), a type of metallic electrode pair whose terminals resemble interlocked fingers [3]. When voltage is applied, an electric field is generated within the substrate. The piezoelectric properties of lithium niobate allow strains to be generated in the presence of electric fields. Applying a sinusoidal voltage leads to a periodic compression-relaxation of the substrate, driving the masses in and out of the substrate plane. It should be noted here that the masses are strategically placed at the antinodes of the generated SAW to maximize out-of-plane drive motion. This strategic placement causes constructive interference, yielding maximum z-axis displacement. The operating principle for a DCMA-based SAW gyroscope, insofar as they use masses to sense gyroscopic precession, is virtually identical to that of a conventional CVG gyroscope; the only difference is the way in which mechanical motion is converted to electrical output (recall that in the CVG case, the proof mass is attached to sensing electrodes that convey electrical information to the sensor output by changing their distance from electrodes that are fixed to a stationary frame). The resulting auxiliary SAWs generated by the propagative motion of the Coriolis masses in the sense axis lead to mechanoelectrical transduction at the receiving (sensing) IDTs. This mechanically induced electric current is proportional to the Coriolis force. The gyroscopic response

from the SAW modes is isolated by means of multiple lock-in amplifiers. The double demodulation process is further described in Section 3.2.

BAW Mode

Waves traveling through the bulk of an elastic substrate are influenced by rotation of the inertial frame. BAWs are described in terms of its longitudinal and transverse components (i.e., *pressure* or *P-waves* and *shear* or *S-waves*, respectively). The polarization of the latter *shear* component has been observed to change with the magnitude of a Coriolis force component. This effect may also be seen on a much larger scale, as particles under the influence of the shear components of seismic events traveling through the Earth were found to act as Foucault pendulums in that their motion is influenced by the rotation of the Earth [4].

As the wavefront of a BAW propagates through the bulk of the material, it will eventually meet a boundary (in the present case, this boundary is a lithium niobate-air interface) and reflect back toward the excitation source, effectively creating a standing wave in a resonating cavity defined by the top and bottom of the substrate. It is conjectured that diffraction effects occur as a result of this standing wave, causing other diffraction waves to appear elsewhere on the device. When driven at the SAW resonance, diffraction waves from the BAW standing wave may excite the distributed Coriolis mass array and produce auxiliary SAWs. This is why some observed SAW effects in sometimes qualified as *bulk-excited* SAW [1]. Other diffraction components manifest at the sense ports .

It was previously established that the polarization of shear waves is influ-

enced by the Coriolis force, and by extension, an applied external angular rotation. The output current of the sensing IDTs is related to the angle difference between the IDTs and the incoming shear wave. In effect, this allows the output signal of the sensing IDTs to carry information about any externally imposed angular rate. As in the SAW case, the IDT output is subjected to a double demodulation scheme to isolate the gyroscopic response, a process which is detailed in Section 3.2.

CHAPTER 3

EXPERIMENTAL METHODS

3.1 Testbed Integration

Prior to the current work, the test setup consisted of the SAW device mounted on the rate table inside the temperature chamber, and multiple data cables feeding out to a lock-in amplifier instrument. Since the commercial lock-in amplifier used (Zurich UHFLI) was too bulky to fit in the temperature chamber, data cables connecting the sample and the lock-in amplifier prevented full revolutions of the rate table. Because of this constraint, gyroscopes are tested by dithering the sample, which here simply refers to “waggling” or periodic back-and-forth oscillatory motion. This is achieved by one of two testing schemes. The first, as described above, involves mounting the sample directly to a rate table. The second involves a PASCO mechanical wave driver (Figure 3.1). A small mag-



Figure 3.1: PASCO Mechanical Wave Driver

net was mounted to the end of the moving pin on the instrument. A magnet

was also placed at the backside of the gyroscope PCB. In this scheme, the moving magnet periodically induces a torque on the PCB, which causes an angular acceleration about the gyroscope's sense axis.

To fix some of the constraints found in the current setup, a new test setup was proposed, one where the demodulation hardware would sit inside the chamber, freeing up the sample to continuously rotate. The new lock-in amplifier, the Moku:Lab by Liquid Instruments, was chosen mainly due to its small form factor, allowing it to sit comfortably on the rate table inside the temperature chamber and rotate with the sample. The new setup (Figures 3.3 and 3.2) requires that a mount be designed to affix the PCB containing the gyroscope sample directly above the center of rotation. Unlike the Zurich UHFLI, the Moku:Lab transmits

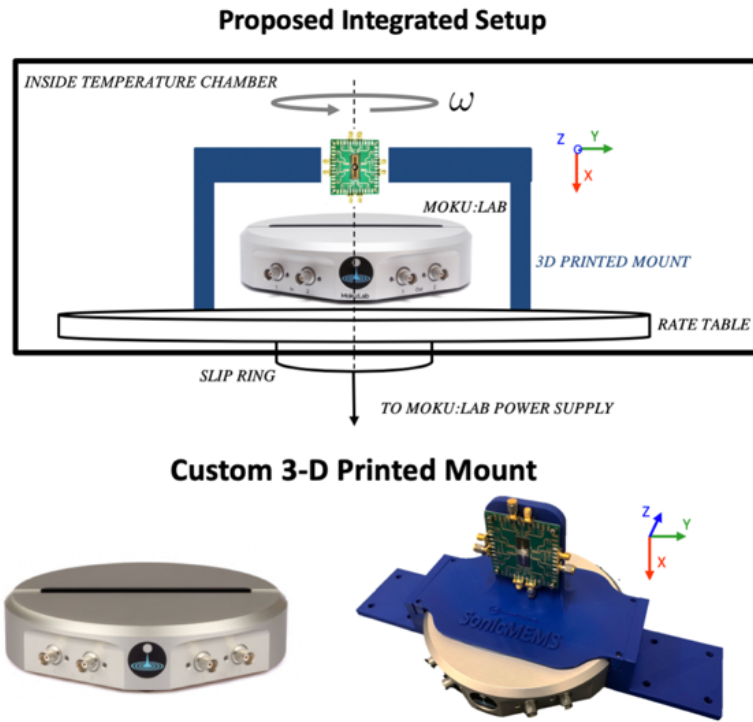


Figure 3.2: Proposed integrated setup

its data wirelessly to a base computer over a local WiFi connection, eliminating

the need for data cables coming out of the test chamber. To power the instrument, power rails were routed through a slip ring located at the bottom of the rate table. The purpose of the slip ring is to maintain electrical connections between the rate table and stationary environment despite the fast rotation of one inertial frame of reference with respect to the other. However, it was found in previous work that data cannot be reliably routed through the slip ring due to unwanted noise.

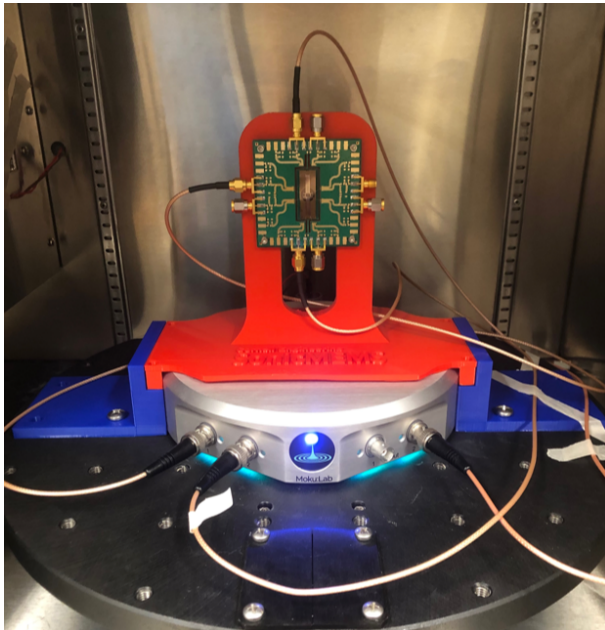


Figure 3.3: Test setup mounted on rate table

There are several tradeoffs to this new, untethered setup. First, unlike the Zurich UHFLI, the Moku:Lab only has a single hardware demodulator on board. This means that the first demodulation is performed *in situ* on the Moku:Lab hardware, while the second demodulation is performed digitally in MATLAB as a post-processing step. The latter, digital demodulation step is especially challenging to implement in the current case, especially given Nyquist constraints in digital signal processing. Two methods for this digital demodu-

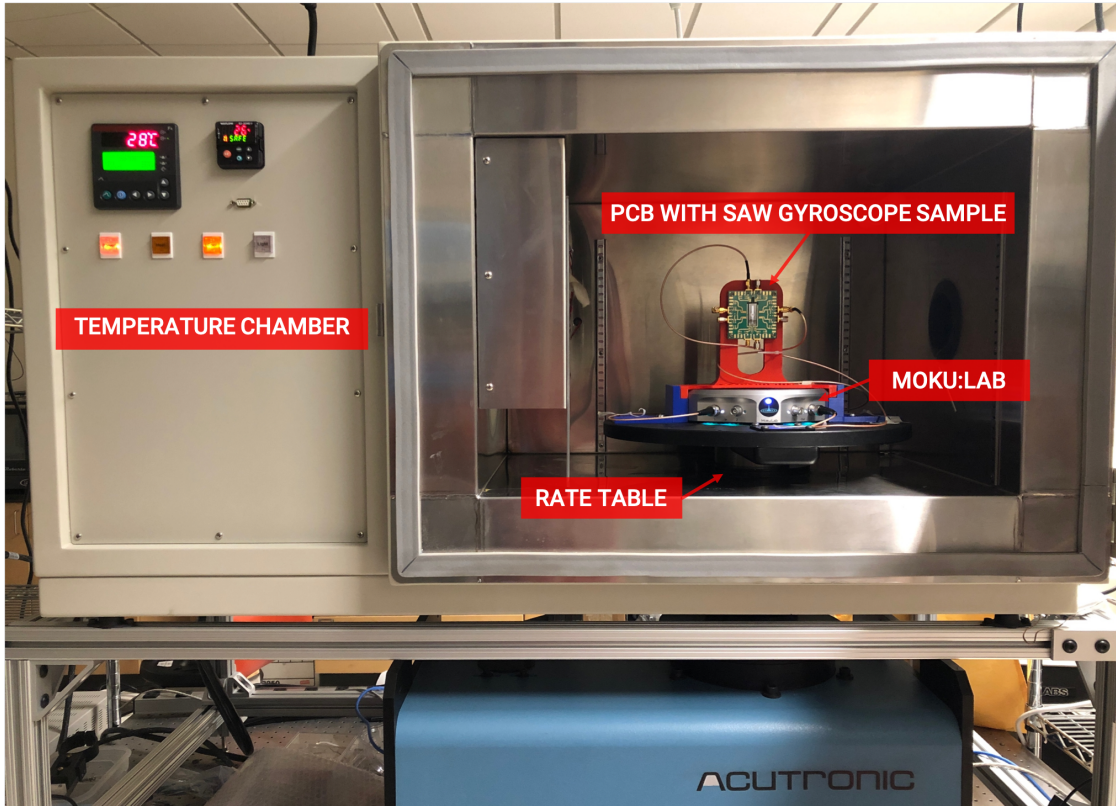


Figure 3.4: Fully integrated Moku:Lab testing framework

lation step are described in the next section.

3.2 Isolating Gyroscopic Response with Double Demodulation

The piezoelectric substrate modulates the two frequencies in a manner similar to amplitude modulation. This effectively creates frequency components at the carrier (drive) frequency f_D , and its sidebands $f_D \pm f_{RT}$, where f_{RT} is the frequency at which the rate table is perturbed. In order to separate the signal due to rate table motion from the drive signal, a lock-in amplifier was used to separate the two contributing frequency components. A double demodulation scheme

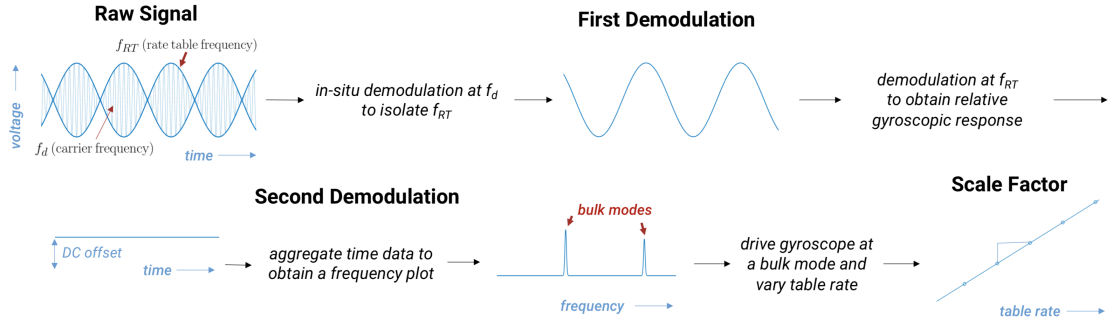


Figure 3.5: Double demodulation scheme

is employed to isolate the raw gyroscopic response from this mixed-frequency signal (Figure 3.5).

First Demodulation

The first demodulation of the raw sense signal is performed *in situ* with the Moku:Lab apparatus with the drive frequency of the gyroscope acting as the local reference signal. The instrument provides one demodulator which may be configured either by the proprietary Moku:Lab iPad app, or programmatically via Python, MATLAB, or LabVIEW interfaces. In this work, a MATLAB interface is used. The resulting demodulated signal represents the amplitude of the carrier signal, or the gyroscopic response at a zero-rate bias. These peaks usually manifest at the millivolt (mV) order of magnitude. This was achieved by performing a demodulation operation on the signal at the drive frequency.

$$V_{signal} = \cos(2\pi f_d t) \cdot \cos(2\pi f_{RT} t) \quad (3.1)$$

This operation uses a mixer which shifts the existing spectra to DC and create a copy at twice the demodulation frequency. Recall that since the demodulation frequency is the drive frequency, we expect to see peaks at 0 Hz and $2f_d$. The DC component is separated from the $2f_d$ component by means of a low pass filter yielding a sinusoidal waveform at f_{RT} with some DC offset.

For an ideal sensor, the output of this operation should consist of a sinusoidal waveform corresponding to the dither frequency of the rate table. For instance, if the rate table were dithered at 3 Hz and the SAW gyroscope was driven at 100 MHz, a demodulation operation with the local oscillator set to 100 MHz would be performed on the signal coming from the sense port, yielding a 3 Hz waveform at the demodulated output (Figure 3.5).

Second Demodulation

A second demodulation operation is then applied, this time at the dither frequency, to create plots representing the relative response of the gyroscope. The primary hardware limitation to the fully integrated setup is that the Moku:Lab, unlike the Zurich UHFLI, only has one hardware demodulator. This means that the second demodulation is to be performed digitally, in software.

Aggressive low pass filtering is first applied before frequency mixing to isolate the 10 Hz component from the rest of the spectra and remove harmonic modes as a result of unwanted aliasing effects. The low-pass filter was implemented using the MATLAB Signal Analyzer Toolbox with 100 dB stopband attenuation and a steepness of 0.99.

As per Nyquist's Sampling Criterion, the sampling frequency of the signal

to be digitally demodulated should be at least twice the highest frequency component of interest to subdue any potential aliasing effects. This criterion is addressed naturally by virtue of the already-low frequency at which the sample is able to be dithered. In the current application, for instance, the hardware lock-in amplifier creates two frequency components one at DC and another at $2f_{RT}$. The minimum sampling frequency should therefore be $2f_{RT}$ (conversely, the maximum rate table frequency should be $0.25f_{RT}$). This should not normally be an issue, as it is the case with dithering the rate table that $f_{RT} \ll f_s$ due to the inertial constraints of wagging back-and-forth a substantial mass at a high frequency. This constraint becomes important, however, when performing high-speed rotation tests with the rate table at the 1000 deg/s order, or performing higher frequency dithering with the PASCO wave generator and the magnetic stage setup.

Using a synchronous demodulation scheme by artificially implementing a local oscillator programmatically is especially sensitive to the above Nyquist criteria. However asynchronous demodulation, implemented through peak-to-peak detection, was found to be more easily implementable and produce better results. This method, however, is more prone to the DC shifting effects of frequency drift; this demodulation approach is not robust to the substantial DC offset effects produced by temperature fluctuations (described in Section 3.3.1). After ensuring that the experimental setup yielded a constant DC level, the latter method was ultimately used in the present work.

3.3 Results

BAW Mode Investigation

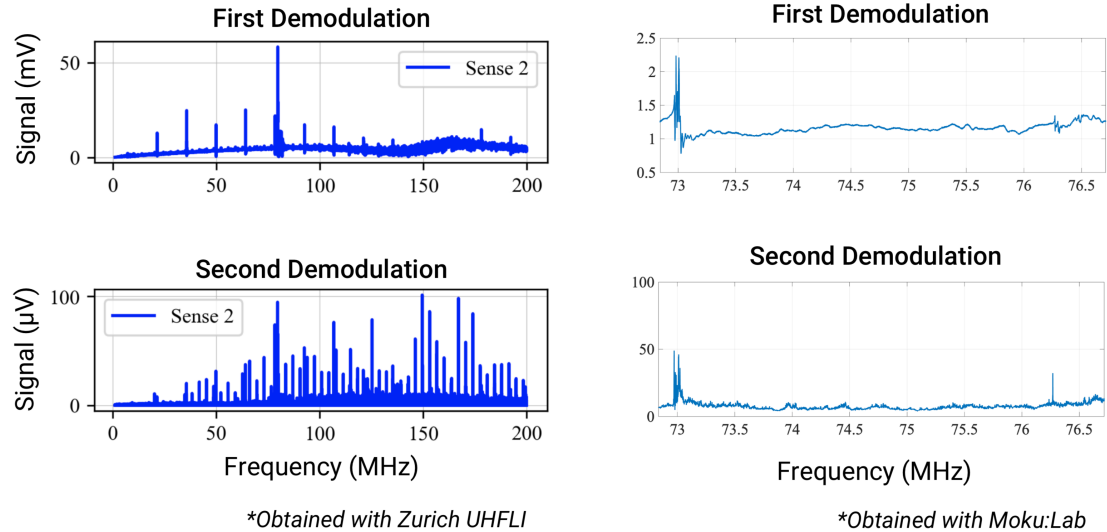


Figure 3.6: Detected bulk modes

Once bulk modes were found using the described double demodulation scheme, the sensitivity of the gyroscope may be determined by driving the gyroscope at a bulk mode, then varying the dither rate of the rate table. Creating an amplitude vs. dither rate plot should yield a linear trend whose slope is the gyroscope scale factor.

SAW Mode Investigation

In the present device, the DCMA masses are placed in such a way that they coincide with the antinodes of a diffracted bulk wave at 80 MHz. The output of the Drive Out port should, in theory, show a signal maximum (corresponding to maximum SAW amplitude) at 80 MHz.

This test is normally performed by a network analyzer (i.e. Keysight E5061B network analyzer). However, this instrumentation is not able to operate *in situ* due to its size and data cable connection constraints. For this reason, the Moku:Lab had to be programmed to mimic the functionality of a network analyzer. One of the built-in instruments built into the Moku:Lab is a spectrum analyzer, which outputs the power of a signal given a drive frequency. A MATLAB script was written using the proprietary moku-MATLAB toolbox to assemble an S_{21} plot by conducting a frequency sweep at the drive input and measuring the corresponding output power of each frequency step. A coarse sweep is first performed to roughly find the location of the peaks. A peak detection algorithm is then applied to set the parameters for a finer sweep that is able to more precisely locate peaks at a 1 kHz resolution (Figure 3.7). The sample mea-

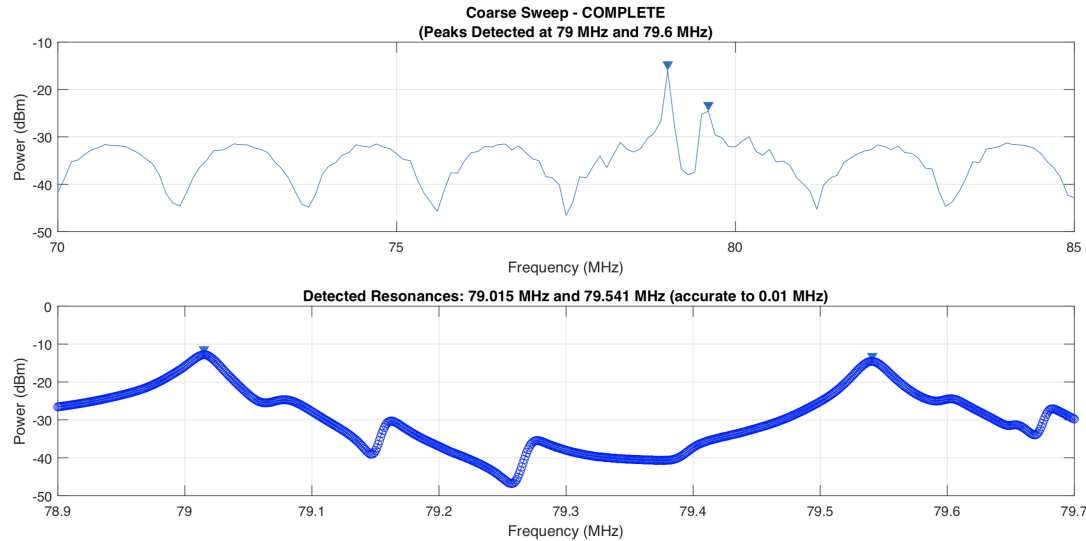


Figure 3.7: SAW modes detected with Moku:Lab setup

sured showed minimal power loss (maximal transmission) at 79.014 MHz and 79.543 MHz, consistent with the desired 80 MHz design. The insertion loss was

derived from the S_{21} parameter and is expressed in dB by:

$$L_{insertion} = -20 \log_{10} |S_{21}| \quad (3.2)$$

SAW modes were found at 79.016 MHz and 79.541 MHz with insertion losses of -14.8 dB and -17.7 dB, respectively (Figure 3.7). These results are consistent with the intended 80 MHz design.

3.3.1 Sources of Noise

A significant part of this work consists of efforts to mitigate to a reasonable degree, or completely eliminate, various sources of environmental noise that adversely affects the results. The two main sources of noise, discussed in this subsection, are thermomechanical and motion artifact.

Thermomechanical Effects

Initially, experiments were conducted in the temperature chamber at 22 C. For this subset of trials, a low frequency oscillation on the order of 100 mHz affecting the DC offset of the demodulated signal was uncovered. Driving the gyroscope at different frequencies found that this effect only occurs at the shear modes and increases in amplitude at higher frequencies (Figure 3.8). Further investigation as to the source of this noise proves that this oscillation was caused by temperature oscillations in the chamber.

At first, experiments were conducted at the textbook value of room temper-

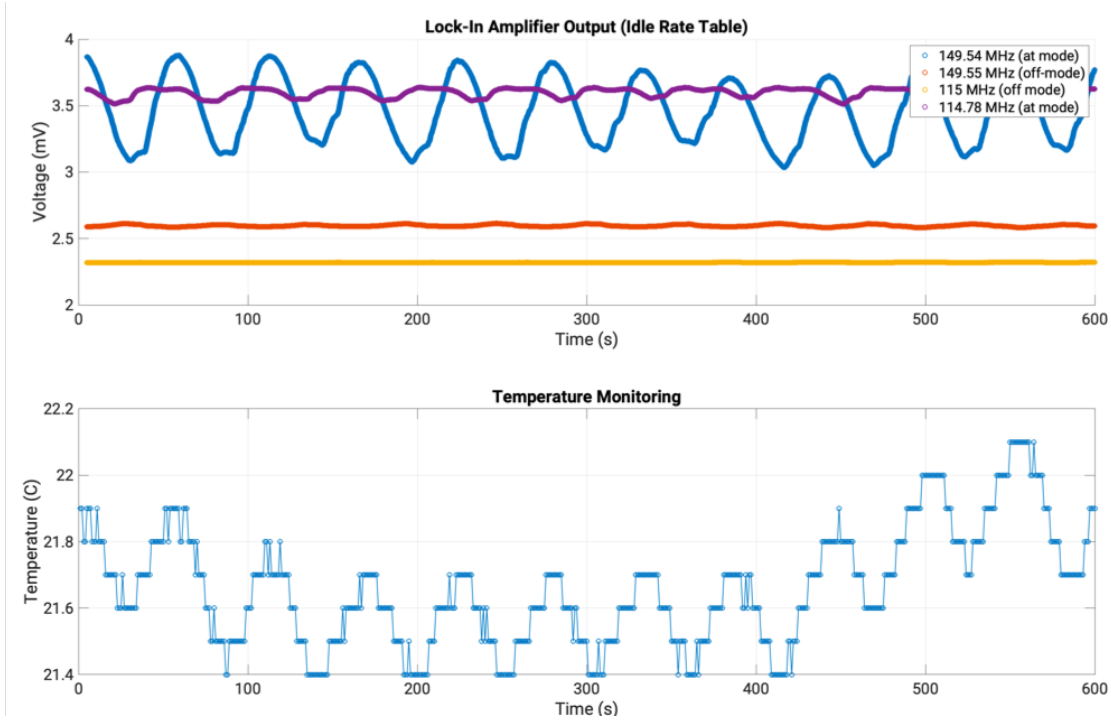


Figure 3.8: Temperature driven low frequency oscillations

ature (22°C). However, the temperature of the local environment was much higher than this baseline. This led to the temperature chamber having to constantly correct the internal temperature by periodically cooling down and heating up the sample. Operating the chamber at a higher temperature ($30\text{-}35^{\circ}\text{C}$) was found to eliminate this oscillation and stabilize the unwanted DC oscillations.

Cable Motion

The first several dither tests with the new integrated setup yielded a very clear signal with suspiciously high SNR values. Further investigation proved that this signal arose as a result of unwanted RF cable motion artifact. This is a

deceptive false positive, since the cables are perturbed at the same frequency at which the rate table is dithered, yielding a similar waveform to what one might expect the demodulated SAW gyroscope output to appear. To eliminate this signal, all RF cables were secured to the rotation stage for future tests.

CHAPTER 4

CONCLUSION

It was established that gyroscopic sensing may be realized on a solid-state piezoelectric substrate by taking advantage of coexisting surface and bulk acoustic wave effects generated by IDTs [5]. It was shown that the polarization of the shear component of each is influenced by the Coriolis effect; a change that may be picked up by the sensing IDTs.

The bulk of the work for this project consisted of the creation of an *in situ* inertial testbed to supplement the development of the described solid-state gyroscope. The inertial testbed is capable of conducting an initial demodulation operation within the confines of the rate table, allowing the sample to rotate freely. A double demodulation scheme is realized in MATLAB to isolate the raw gyroscopic response due to a back-and-forth dither. Additional MATLAB scripts (provided in Appendices B and C) were created to conduct a variety of experiments by simultaneously interfacing with the rate table and Moku:Lab.

This report showed preliminary results obtained with this new, integrated setup. While further investigation of gyroscopic scale factor at each detected mode is needed to determine whether the sample functions as a gyroscope, these results indicate the device's veritability as a solid-state inertial sensor.

Future Work

Obtain reliable scale factor plots with integrated setup. Further work is needed to obtain scale factor plots with the inertial rate table. Unlike the PASCO magnetic stage setup, the inertial rate table is unable to achieve high dither rates.

Attempts to obtain the gyroscopic scale factor using the latter, integrated setup yielded noisy outputs due to the limited range of achievable dither rates.

Add another hardware demodulation stage inside rate table. It was established that digital demodulation is challenging to implement, and is susceptible to unwanted aliasing effects (if using synchronous demodulation) or unwanted DC offset (if using asynchronous demodulation). An ideal solution would be to introduce another hardware demodulation stage prior to entering the Moku:Lab.

Make integrated testbed fully remotely accessible. Further work is also needed to make the inertial testbed even easier to use. Currently, it is necessary for an operator to be present in the lab space to begin inertial tests. This is primarily because the lab computer can only connect to one wireless network at a time; connecting to the Moku:lab WiFi network will disconnect the computer from the internet. Connecting a WiFi dongle will enable the computer to connect to multiple networks, allowing the testbed to be remotely accessed from anywhere on campus. A webcam will also be fixed inside the temperature chamber to allow researchers to monitor the sample throughout the experiment.

REFERENCES

- [1] B. Davaji, V. Pinrod, S. Kulkarni, and A. Lal, "Towards a surface and bulk excited SAW gyroscope," in *2017 IEEE International Ultrasonics Symposium (IUS)*, pp. 1–4, IEEE, 2017.
- [2] W. Wang, H. Oh, K. Lee, S. Yoon, and S. Yang, "Enhanced sensitivity of novel surface acoustic wave microelectromechanical system-interdigital transducer gyroscope," *Japanese Journal of Applied Physics*, vol. 48, no. 6S, p. 06FK09, 2009.
- [3] A. Ruyack, B. Davaji, S. Kulkarni, and A. Lal, "Characterization of graphene electrodes as piezoresistive SAW transducers," in *2017 IEEE International Ultrasonics Symposium (IUS)*, pp. 1–4, IEEE, 2017.
- [4] R. Snieder, C. Sens-Schönfelder, E. Ruigrok, and K. Shiomi, "Seismic shear waves as Foucault pendulum," *Geophysical Research Letters*, vol. 43, no. 6, pp. 2576–2581, 2016.
- [5] V. Pinrod, B. Davaji, and A. Lal, "Coexisting Surface and Bulk Gyroscopic Effects," in *2018 IEEE International Ultrasonics Symposium (IUS)*, pp. 1–4, IEEE, 2018.

APPENDIX A

SUGGESTED EXPERIMENTAL PROCEDURES

A.1 Detecting SAW Modes

This experiment performs frequency sweeps and peak detection to determine the SAW modes of a sample at a 1 kHz resolution.

1. Set the temperature chamber to 35 °C. Allow a couple hours for the temperature inside the chamber to stabilize before performing any tests.
2. Connect Output Channel 1 of the Moku:Lab to the Drive In port on the SAW gyroscope sample.
3. Connect Input Channel 2 of the Moku:Lab to the Drive Out port on the SAW gyroscope sample. The Sense 1 and Sense 2 ports should be left floating, while all other ports should be grounded.
4. Power on the Moku:Lab and secure the temperature chamber.
5. An orange light will be visible through the observation window while the Moku:Lab is initializing. When the white light appears, connect to the Moku:Lab WiFi network (Moku-000645) on the lab computer.
6. Run `find_resonances.m`. Allow roughly 20 minutes for the program to complete.

A.2 Detecting Bulk Modes

This experiment conducts frequency sweeps at a 10 Hz rate table dither frequency to investigate bulk modes.

1. Set the temperature chamber to 35 °C. Allow a couple hours for the temperature inside the chamber to stabilize before performing any tests.
2. Connect Output Channel 2 of the Moku:Lab to the Drive In port on the SAW gyroscope sample.
3. Connect Input Channel 1 of the Moku:Lab to either the Sense 1 or Sense 2 ports on the SAW gyroscope sample. The Drive Out port should be left floating, while all other ports should be grounded.
4. Connect Input Channel 1 of the Moku:Lab to either the Sense 1 or Sense 2 ports on the SAW gyroscope sample. The Drive Out port should be left floating, while all other ports should be grounded.
5. Power on the Moku:Lab and secure the temperature chamber.
6. An orange light will be visible through the observation window while the Moku:Lab is initializing. When the white light appears, connect to the Moku:Lab WiFi network (Moku-000645) on the lab computer.
7. Open `RT_ditherTest.m`.
8. Set the desired experiment parameters. Available fields include *starting frequency*, *frequency step size*, *ending frequency*. The researcher may also specify an optional descriptor, which will be incorporated into the `.mat` filename at the conclusion of the experiment (along with the date and chosen experiment parameters).

9. Allow several days for the experiment to complete. The runtime will vary depending on the experimental parameters.
10. Load the First and Second Demodulation Plot Generation code (Listing B.1) and replace the file name with the .mat file generated from the previous step.
11. Running the script will yield first and second demodulation plots.

A.3 Determining Scale Factor

This experiment varies the dither rate of the rate table and drives the gyroscope at a desired bulk mode to extract gyroscopic scale factor.

1. Set the temperature chamber to 35 °C. Allow a couple hours for the temperature inside the chamber to stabilize before performing any tests.
2. Connect Output Channel 2 of the Moku:Lab to the Drive In port on the SAW gyroscope sample.
3. Connect Input Channel 1 of the Moku:Lab to either the Sense 1 or Sense 2 ports on the SAW gyroscope sample. The Drive Out port should be left floating, while all other ports should be grounded.
4. Connect Input Channel 1 of the Moku:Lab to either the Sense 1 or Sense 2 ports on the SAW gyroscope sample. The Drive Out port should be left floating, while all other ports should be grounded.
5. Power on the Moku:Lab and secure the temperature chamber.

6. An orange light will be visible through the observation window while the Moku:Lab is initializing. When the white light appears, connect to the Moku:Lab WiFi network (Moku-000645) on the lab computer.
7. Open `RT_scaleFactor.m`.
8. Set a desired drive frequency (this should be one of the detected bulk modes) and the rate table frequency (suggested rate table frequency is 10 Hz). The researcher may also specify an optional descriptor, which will be incorporated into the `.mat` filename at the conclusion of the experiment (along with the date and chosen experiment parameter).
9. Allow at least two hours for the experiment to complete.
10. Load the Scale Factor Determination code (Listing B.2) and replace the file name with the `.mat` file generated from the previous step.
11. Running the script will yield amplitude vs. dither rate plots from which the scale factor may be extracted.

APPENDIX B

MOKU:LAB MATLAB INTERFACE CODE LISTINGS

```
clear all
clc
m = MokuSpectrumAnalyzer('192.168.73.1');

lo_freq = 70e6
hi_freq = 85e6
step_size = (hi_freq-lo_freq)/150

power = []
freq = []

power2 = []
freq2 = []

m = MokuSpectrumAnalyzer('192.168.73.1');

% Set a start/stop frequency of 30MHz - 50MHz
%m.set_span(lo_freq,hi_freq);

% Set the window function to be "Hanning"
m.set_window('hanning');

% Set the resolution bandwidth to 100kHz
% Note this could be rounded up to the nearest
% possible RBW for your frequency span
m.set_rbw('rbw', 50e3);

m.gen_sinewave(1, 2.0, 100e6);
m.set_dbmscale('dbm',true);

figure(1)
hold on
grid on

tic
for x = lo_freq:step_size:hi_freq
    m.set_span(x, x+1)
    m.gen_sinewave(1, 2.0, x)
    try
        data = m.get_data('timeout',10);
        d1 = data.ch2(1);
        %fs = data.frequency(1);
        power = [power d1];
        freq = [freq x];
        subplot(2,1,1)
        plot(freq/1e6,power-30, '-o', 'Color', 'b')
        title('Coarse Pass - DETECTING PEAKS')
        xlabel('Frequency (MHz)')
        ylabel('Power (dBm)')
        drawnow
    catch e
        e
    end
end
```

```

[psor,lsor] = findpeaks(power-30,freq,'SortStr','descend','NPeaks',2)
;

findpeaks(power-30,freq/1e6,'SortStr','descend','NPeaks',2)
title({'Coarse Sweep - COMPLETE', ['(Peaks Detected at ', num2str(min
(lsor)/1e6), ' MHz and ', num2str(max(lsor)/1e6), ' MHz)']})
xlabel('Frequency (MHz)')
ylabel('Power (dBm)')

for x = min(lsor)-step_size:1e3:max(lsor)+step_size
    m.set_span(x, x+1)
    m.gen_sinewave(1, 2.0, x)
    try
        data = m.get_data('timeout',10);
        d1 = data.ch2(1);
        %fs = data.frequency(1);
        power2 = [power2 d1];
        freq2 = [freq2 x];

        subplot(2,1,2)
        plot(freq2/1e6,power2-30, '-o', 'Color', 'b')
        xlabel('Frequency (MHz)')
        ylabel('Power (dBm)')
        title({'Second Pass - IN PROGRESS', ['(Executing Fine Sweep
from ', num2str((min(lsor)-step_size)/1e6), ' MHz to ', num2str((
max(lsor)+step_size)/1e6), ' MHz)']})
        drawnow
    catch e
        e
    end
end

[psor,lsor] = findpeaks(power2-23,freq2,'SortStr','descend','NPeaks',
,2);
findpeaks(power2-23,freq2/1e6,'SortStr','descend','NPeaks',2)
hold on
plot(freq2/1e6,power2-18, '-o', 'Color', 'b')
title(['Detected Resonances: ', num2str(lsor(1)/1e6), ' MHz and ',
num2str(lsor(2)/1e6), ' MHz (accurate to 0.01 MHz)'])
xlabel('Frequency (MHz)')
ylabel('Power (dBm)')

toc

```

Listing B.1: find_resonances.m

```

clear
clc
FREQ = [];
DATA_10 = [];
DATA_20 = [];
DATA_30 = [];

 $\% \text{ SET EXPERIMENT PARAMETERS}$ 
 $\%$ -----
LO_FREQ = 96.8e6;
HI_FREQ = 97.8e6;
STEP_FREQ = 1e3;
DESCRIPTOR = "rtidither";
 $\%$ -----
TITLE_STRING = string(date) + "_" + num2str(LO_FREQ) + "_" + num2str(
    STEP_FREQ) + "_" + num2str(HI_FREQ) + DESCRIPTOR;
 $\% \text{ CONFIGURE RATE TABLE}$ 
acul = openAcu1();
setAcu1(acul, ':MODE:POSITION 1')
pause(10);
setAcu1(acul, ':MODE:SYNTHESIS 1')
setAcu1(acul, ':CONFIGURE:OSCILLATOR 1,ENABLE,2.0,0.102,RATE,
    LOGARITHMIC')
pause(5);
setAcu1(acul, ':DEMAND:OSCILLATOR 1,10,3,90')
disp('RATE TABLE INITIALIZED')

 $\% \text{ CONFIGURE MOKU}$ 
 $\% \text{ Connect to your Moku and deploy the desired instrument}$ 
m = MokuLockInAmp('192.168.73.1');
m.set_demodulation('internal','frequency',114.7778e6);
m.set_lo_output(2.0,114.7778e6,0);

m.set_outputs('r','sine')

m.set_monitor('A','I');
m.set_monitor('B','Q');

 $\% \text{ PERFORM MEASUREMENTS}$ 
for amp = [10 20 30]
    setAcu1(acul, ":DEMAND:OSCILLATOR 1," + num2str(amp) + ",3,90")
    for freq = LO_FREQ:STEP_FREQ:HI_FREQ
        try
            m.set_demodulation('internal','frequency',freq,
                'output_amplitude', 2.0);
            m.set_lo_output(2.0,freq,0);
            m.set_timebase(0,6);

            data = m.get_data();

            if amp == 10
                FREQ = [FREQ freq];
                DATA_10 = [DATA_10; data];

            elseif amp == 20
                DATA_20 = [DATA_20; data];

            else
                DATA_30 = [DATA_30; data];
            end

            figure(1)
            plot(data.time, data.ch1, data.time, data.ch2)

```

```

    title(freq/1e6)
    drawnow
    catch e
        setAcu1(acu1, ':DEMAND:OSCILLATOR 1,0,1,90')
        save(TITLE_STRING + ".mat",'DATA_10','DATA_20', 'DATA_30',
        'FREQ')
        fprintf("ERROR AT %3.2d MHz/n, %d amplitude", freq, amp)
        break
    end
end
save(TITLE_STRING + ".mat",'DATA_10','DATA_20', 'DATA_30','FREQ')

setAcu1(acu1, ':DEMAND:OSCILLATOR 1,0,1,90')
pause(5);
closeAcu1(acu1)

```

Listing B.2: RT_ditherTest.m

```

clear
clc

DATA = [];

%% SET EXPERIMENT PARAMETERS
%-----
DRIVE_FREQ = 76.27E6;
RT_FREQ = 10;
DESCRIPTOR = "rttdither_SCALEFACTORMEAS";
%-----
TITLE_STRING = string(date) + " " + num2str(DRIVE_FREQ/1.0e6) + "MHz_
" + num2str(RT_FREQ) + "hz_" + DESCRIPTOR;
%% CONFIGURE RATE TABLE
acul = openAcul();
setAcul(acul, ':MODE:POSITION 1');
pause(10);
setAcul(acul, ':MODE:SYNTHESIS 1');
setAcul(acul, ':CONFIGURE:OSCILLATOR 1,ENABLE,2.0,0.102,RATE,
LOGARITHMIC');
pause(5);
setAcul(acul, [:DEMAND:OSCILLATOR 1,10,3,90']);
disp('RATE TABLE INITIALIZED')

%% CONFIGURE MOKU
% Connect to your Moku and deploy the desired instrument
m = MokuLockInAmp('192.168.73.1');
m.set_demodulation('internal','frequency',114.7778e6);
m.set_lo_output(2.0,114.7778e6,0);

m.set_outputs('r','sine');

m.set_monitor('A','I');
m.set_monitor('B','Q');

%% PERFORM MEASUREMENTS
for amp = [1 2 3 4 5]
    setAcul(acul, [:DEMAND:OSCILLATOR 1,"+num2str(amp)+","+num2str(
RT_FREQ)+"",90"]);
    freq = DRIVE_FREQ
    pause(10)
    try
        m.set_demodulation('internal','frequency',freq,
output_amplitude', 2.0);
        m.set_lo_output(2.0,freq,0);
        m.set_timebase(0,6);

        data = m.get_data();
        DATA = [DATA; data];

        figure(1)
        plot(data.time, data.ch1, data.time, data.ch2)
        title(amp)
        drawnow
    catch e
        setAcul(acul, ':DEMAND:OSCILLATOR 1,0,1,90');
        save(TITLE_STRING + ".mat",'DATA');
        fprintf("ERROR AT %d amplitude", amp)
        break
    end
end

```

```
save(TITLE_STRING + ".mat",'DATA');
disp("TEST COMPLETED SUCCESSFULLY! DATA SAVED.");
setAcu1(acu1, ':DEMAND:OSCILLATOR 1,0,1,90');
pause(5);
closeAcu1(acu1)
```

Listing B.3: RT_scaleFactor.m

APPENDIX C

POST-PROCESSING MATLAB CODE LISTINGS

```

clear
clc

load('16-Apr-2019_70MHz_1kHz_80MHz_10hz_rtdither.mat')
AMP1 = [];
AMP2 = [];

%forloop max
%n = 5
n = length(DATA);

time = DATA(1).time;
fs = length(time)/max(time)
freq_RT = 10;

S = sin(2*pi*freq_RT*time);
C = cos(2*pi*freq_RT*time);

for i = 1:n
    i1 = DATA(i).ch1-mean(DATA(i).ch1);
    q1 = DATA(i).ch2-mean(DATA(i).ch2);

    i1_filt = lowpass(DATA(i).ch1, freq_RT , fs,'Steepness',0.999);
    q1_filt = lowpass(DATA(i).ch2, freq_RT , fs,'Steepness',0.999);

    %Calculate R
    r1 = sqrt(i1_filt.^2+q1_filt.^2);
    %r1 = r1-mean(r1);
    r1_unfiltered = sqrt(DATA(i).ch1.^2+DATA(i).ch2.^2);
    r1_unfiltered = r1_unfiltered-mean(r1_unfiltered);
    %Build 1st Demod Frequency Plots
    ampl1 = mean(r1);

    %% Build 2nd Demod Frequency Plots - SYNCHRONOUS METHOD
    i2 = r1.*S*1e-6;
    q2 = r1.*C*1e-6;

    i2_filt = lowpass(i2, 0.0001,'Steepness',0.999);
    q2_filt = lowpass(q2, 0.0001,'Steepness',0.999);

    r2 = sqrt(i2_filt.^2+q2_filt.^2);
    %% Build 2nd Demod Frequency Plots - ASYNCHRONOUS METHOD

    [~, offset] = envelope(r1, 800, 'peak');
    amp2 = peak2peak(r1_unfiltered(5000:12000));

    AMP1 = [AMP1 ampl1];
    AMP2 = [AMP2 amp2];
    clc
    display(i)

    figure(1)
    plot(r1(5000:12000)-offset(5000:12000))
    hold on
    grid on
    drawnow
    end

```

```

% Add this at the beginning
% Change default axes fonts.
set(0,'DefaultAxesFontName', 'Arial')
set(0,'DefaultAxesFontSize', 30)
set(0,'DefaultAxesFontWeight', 'Bold')

% Change default text fonts.
set(0,'DefaultTextFontname', 'Arial')
set(0,'DefaultTextFontSize', 30)

figure(2)
subplot(2,1,1)
plot(FREQ(1:n)./1e6, AMP1.*1e3, 'LineWidth', 2)
xlabel('Frequency (MHz)')
ylabel('Amplitude (mV)')
title('First Demodulation')
grid on

subplot(2,1,2)
plot(FREQ./1e6, AMP2.*1e6, 'LineWidth', 2)
xlabel('Frequency (MHz)')
ylabel('Amplitude (uV)')
title('Second Demodulation')
grid on

```

Listing C.1: First and Second Demodulation Plot Generation

```

clear
clc

% Add this at the beginning
% Change default axes fonts.
set(gcf,'color','w');
set(0,'DefaultAxesFontName', 'Adobe Caslon Pro')
set(0,'DefaultAxesFontSize', 30)
set(0,'DefaultAxesFontWeight')

% Change default text fonts.
set(0,'DefaultTextFontname', 'Arial')
set(0,'DefaultTextFontSize', 30)

load('21-Apr-2019_76.27MHz_10hz_rtdither_SCALEFACTORMEAS.mat')
AMP1 = [];
AMP2 = [];

%forloop max
%n = 5

time = DATA(1).time;
fs = length(time)/max(time)
freq_RT = 10;

for i = 1:length(DATA)

    i1 = DATA(i).ch1;
    q1 = DATA(i).ch2;
    i1_filt = lowpass(DATA(i).ch1, freq_RT, fs/2,'Steepness',0.999);
    q1_filt = lowpass(DATA(i).ch2, freq_RT, fs/2,'Steepness',0.999);

    %Calculate R
    r1 = sqrt(i1_filt.^2+q1_filt.^2);
    r1_unfiltered = sqrt(i1.^2+q1.^2);
    if i==1
        data1 = r1_unfiltered;
    elseif i==2
        data2 = r1_unfiltered;
    elseif i==3
        data3 = r1_unfiltered;
    elseif i==4
        data4 = r1_unfiltered;
    elseif i==5
        data5 = r1_unfiltered;

    end

    %Build 1st Demod Frequency Plots
    amp1 = mean(r1);

    %% Build 2nd Demod Frequency Plots - ASYNCHRONOUS METHOD

    [~, offset] = envelope(r1, 800, 'peak');
    amp2 = peak2peak(r1_unfiltered(5000:12000));

    AMP1 = [AMP1 amp1];
    AMP2 = [AMP2 amp2];
    clc
    display(i)

```

```

figure(1)
plot(time(5000:12000), r1(5000:12000)-offset(5000:12000), '
LineWidth', 2)
legend('1',' ','2',' ','3',' ','4',' ','5')
hold on
grid on
drawnow
end

figure(2)
set(gcf, 'color', 'w');

plot(AMP2, 'LineWidth', 2)
xlabel('Rate')
ylabel('Amplitude (mV)')
title('Scale Factor Determination')
grid on

```

Listing C.2: Scale Factor Determination